Available online at www.sciencedirect.com
ScienceDirect
Trans. Nonferrous Met. Soc. China 24(2014) 1813−1818
Transactions of Nonferrous Metals Society of China
www.tnmsc.cn

Facile synthesis of tin oxide nanocrystals and their photocatalytic activity

Zhi-qian JIA[1], Hui-jie SUN[1], Yan WANG[1], Tian-li ZHEN[1], Qing CHANG[1,2]

1. College of Chemistry, Beijing Normal University, Beijing 100875, China;
2. Science and Technology on Remanufacturing Laboratory, Academy of Armored Forces Engineering, Beijing 100072, China

Received 26 June 2013; accepted 23 January 2014

Abstract: Tin oxide nanocrystals with diameters smaller than 10 nm were synthesized using Na_2SnO_3 and CO_2 as reactants and cetyltrimethylammonium bromide (CTAB) as stabilizer under mild conditions. As a mild acidic gas, CO_2 is favorable for the accurate adjustment of pH value of Na_2SnO_3 solution. Stannate salt is stable, cheap and easy in operation. The effects of Na_2SnO_3 concentration, CTAB concentration, aging temperature, and aging time on the nanocrystals were studied. It was found that, with the increasing Na_2SnO_3 concentration, aging temperature and aging time, SnO_2 nanocrystals size decreases. The formation of SnO_2 nanocrystals can be interpreted by electrostatic-interaction mechanism. SnO_2 nanocrystals show high photocatalytic activities in the degradation of Rhodamine B solution. The catalytic activity of small nanocrystals is higher than that of large ones.
Key words: tin oxide nanocrystals; facile synthesis; photocatalytic activity

1 Introduction

As a wide band-gap n-type semiconductor (E_g = 3.6 eV at bulk state), tin oxide has drawn considerable attention owing to its various applications such as catalysts for oxidation of organic compounds [1], solid-state gas sensors for reducing gases [2], rechargeable Li-batteries [3,4], optical electronic devices [5], photocatalysts [6]. The size of tin oxide particles has been shown to drastically affect their properties due to surface and/or spacial confinement effects. Various methods have been developed for the synthesis of tin oxide nanocrystals, including thermolysis of organometallic precursors, sol−gel [7], hydrolysis of $SnCl_2$ [8,9] or SnF_2 [10], sonochemistry, and hydrothermal synthesis [11,12]. However, the fabrication of tin oxide nanocrystals with diameter smaller than 10 nm is still a challenge. Recently, WU et al [13] reported a lysteine-assisted hydrothermal route for generating SnO_2 nanocrystals (<10 nm). But the conditions (120−240 °C) are very harsh. JUTTUKONDA et al [14] employed stannate salt, carbon dioxide and fourth-generation dendritic polymers for the synthesis of tin oxide nanocrystals (<10 nm). Nevertheless, the dendritic polymers are very expensive due to the difficulty in synthesis.

In this work, tin oxide nanocrystals with diameters smaller than 10 nm were synthesized using Na_2SnO_3 and CO_2 as reactants and cetyltrimethylammonium bromide (CTAB) as stabilizer under mild conditions. Firstly, Na_2SnO_3 aqueous solution was carbonated by CO_2 to generate stannate acid. Then, CTAB solution was added, which interacted with stannate anions via electrostatic interaction. After aging, filtration, washing, drying and calcinations, tin oxide nanocrystals (<10 nm) were obtained. Compared with strong or moderate acids such as hydrochloric acid, H_2SO_4 or H_3PO_4, CO_2 is a mild acidic gas and is favorable for the accurate adjustment of pH value of Na_2SnO_3 solution, as well as for the emission reduction of greenhouse gas [15]. Meanwhile, in contrast with moisture-sensitive reagents (e.g. tin chloride), stannate salt is stable, cheap and easy in operation. In addition, the CTAB stabilizer is much cheaper than most of the other stabilizers. The effects of Na_2SnO_3 concentration, CTAB concentration, aging temperature, and aging time on the nanocrystals were studied. The photocatalytic activity of the SnO_2 nanocrystals in the degradation of Rhodamine B (RhB, Scheme 1) aqueous solution was evaluated.

Foundation item: Projects (20676016, 21076024) supported by the National Natural Science Foundation of China
Corresponding author: Zhi-qian JIA; Tel: +86-10-58802945; E-mail: zhqjia@bnu.edu.cn
DOI: 10.1016/S1003-6326(14)63258-1

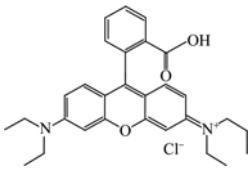

Scheme 1 Rhodamine B

2 Experimental

2.1 Materials

The chemical reagents, including Na_2SnO_3 and CTAB, were in analytical grade and used as-received without further purification. The fresh Na_2SnO_3 solution was prepared with degassed pure water prior to the reaction.

2.2 Preparation of tin oxide

In a typical synthesis, CO_2 gas was bubbled into 250.0 mL of Na_2SnO_3 solution in a stirred tank at ambient temperature until a certain pH was attained. Then CTAB solution was added to precipitate the stannate acid, and the white turbid suspension was aged at design temperature for a certain time. After centrifugation, the as-obtained precipitate was washed with pure water and alcohol, dried at room temperature and then at 110 °C for 2 h. Last, the white powder was calcinated at 150 °C in Muffle furnace for 2 h and at 400 °C for another 2 h to remove CTAB completely.

2.3 Analysis

The products were observed on a transmission electron microscope (JEM 2010, Japan). In each image, more than one hundred particles were measured to determine the average size. The XRD pattern was analyzed by monochromatized Cu K_α incident radiation (Shimadzu XRD−6000). Nitrogen absorption−desorption isotherms were measured at 77 K by a volumetric technique (V-Sorb 4800P, Beijing), and the surface area was calculated by the Brunaner−Emmett−Teller (BET) method.

2.4 Photocatalytic activity

The photocatalytic activities of the SnO_2 nanocrystals in the degradation of RhB aqueous solution were evaluated. First, 50.0 mL of 1×10^{-5} mol/L RhB solution (containing 50.0 mg of SnO_2 sample) was stirred in a vessel (*d*115 mm) for 30 min at room temperature to attain an adsorption−desorption equilibrium. Then, a 500 W high-pressure mercury lamp (Beijing Tianmai Henghui Co. Ltd) was employed to irradiate the stirred RhB solution, and the distance between the lamp and the solution was 45.0 cm. The concentration of RhB was monitored by an UV-vis spectrometer (Cintra 10e, Australia) during UV irradiation.

3 Results and discussion

3.1 Evolution of pH value during carbonation

Figure 1 shows the pH evolution of Na_2SnO_3 solution during carbonation. The pH value drops quickly in the initial period (pH>10) and then declines slowly (8<pH<10). In the initial period, the dissolved CO_2 reacts with the excess alkaline in Na_2SnO_3 reagent, resulting in the rapid decline of pH value. The reactions can be expressed as follows [16]:

$$CO_2+OH^- =HCO_3^- \quad (1)$$

$$HCO_3^-+OH^- =CO_3^{2-}+H_2O \quad (2)$$

Then, with the consumption of OH^-, Na_2SnO_3 hydrolyzes and generates stannate acid and OH^-, leading to the slow decline of pH values. The hydrolyzation of Na_2SnO_3 is written as follows:

$$SnO_3^{2-}+3H_2O=Sn(OH)_4+2OH^- \quad (3)$$

$$2Sn(OH)_4=(OH)_3Sn—O—Sn(OH)_3+H_2O \quad (4)$$

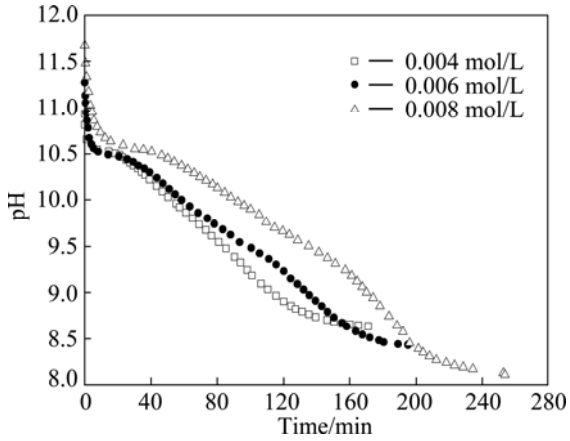

Fig. 1 Evolution of pH values in carbonation for various Na_2SnO_3 concentrations

3.2 Effects of reaction conditions on SnO_2 nanocrystals

The effects of Na_2SnO_3 concentrations were carried out at carbonation pH of 9.0, 0.0033 mol/L CTAB, aging temperature of 110 °C for 24 h, Na_2SnO_3 concentrations of 0.004, 0.006 and 0.008 mol/L, respectively. Figures 2(a), (b) and (c) show that with the increasing Na_2SnO_3 concentration, the SnO_2 nanoparticles size decreases from 5.8 nm to 4.9 nm and 4.5 nm, respectively. Electron diffraction (ED) of nanoparticles exhibits polycrystalline rings (Fig. 2(d)). In contrast, the effects of CTAB concentrations (0.0011, 0.0020 and 0.0033 mol/L) on the nanoparticles are found to be not significant.

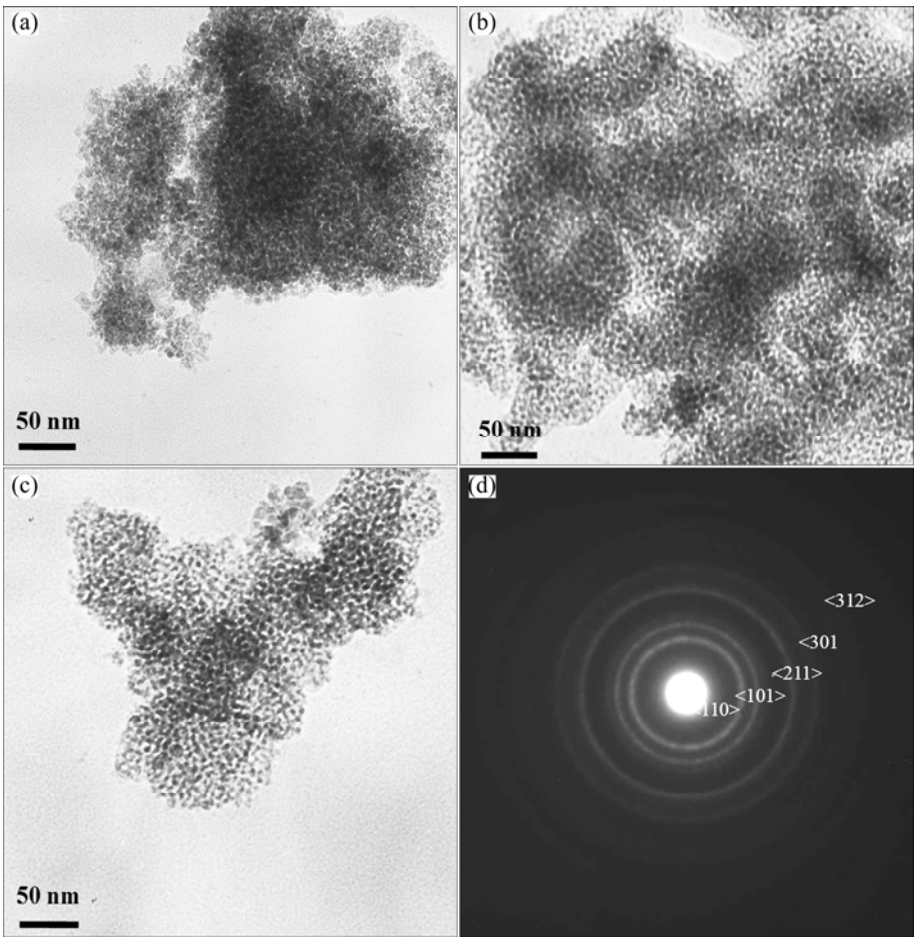

Fig. 2 Effects of Na_2SnO_3 concentrations on SnO_2 nanoparticles: (a) TEM image, 0.004 mol/L; (b) TEM image, 0.006 mol/L; (c) TEM image, 0.008 mol/L; (d) ED pattern, 0.008 mol/L

The effects of aging temperature were conducted at carbonation pH of 10.0, 0.0033 mol/L CTAB, 0.008 mol/L Na_2SnO_3, aging time of 24 h, aging temperature of 25, 70 and 110 °C, respectively. Figure 3 shows that with the increasing aging temperature, the nanoparticles size declines from 16.2 nm to 8.4 nm and 6.7 nm, respectively. The HRTEM analysis (Fig. 3(d)) shows that the interplaner spacing of 1D fringes is 0.335 nm, which is consistent well with the (110) lattice spacing of rutile SnO_2. Figure 4 shows the respective XRD patterns of SnO_2 nanoparticles with 6.7 nm and 16.2 nm in size. The diffraction peaks are in agreement with those of tetragonal tin oxide with rutile structure (PDF00−001−0657, a=4.7382 Å, b=4.7382 Å, c=3.1871 Å). The crystallites size is estimated in terms of the Scherrer equation:

$$D=\frac{k\lambda}{\beta\cos\theta} \tag{5}$$

where λ is wavelength of X–ray (0.154056 nm); k=0.89; β is the full-width-half-maximum (FWHM) of diffraction peak; θ is the diffraction angle. The crystallites sizes are found to be 7.8 nm and 14.2 nm respectively. These values are consistent with the TEM results (6.7 nm and 16.2 nm), indicating that the nanoparticles are single crystals. The BET specific surface areas of the nanocrystals are 480 m^2/g (6.7 nm in size) and 149 m^2/g (16.2 nm in size).

The effects of aging time were studied at carbonation pH of 10.0, 0.0033 mol/L CTAB, 0.008 mol/L Na_2SnO_3, aging temperature of 110 °C, and aging time of 12 h, 24 h and 48 h, respectively. It was found that with rising aging time, the particles size declines from 8.5 nm to 6.7 nm and 6.5 nm, respectively.

3.3 Formation mechanism of SnO_2 nanocrystals

The plausible formation mechanism of SnO_2 nanocrystals is shown in Fig. 5. During carbonation, the solution is alkaline and the as-generated H_2SnO_3 sol is negative charged (denoted as I^-). It interacts with the positively charged head-groups of CTAB (S^+) to form I^-S^+ precipitate. In the subsequent aging period, the H_2SnO_3 sol protected by the surrounding CTAB molecules further condenses. After washing, drying and calcinations, CTAB is removed and SnO_2 nanocrystals are obtained.

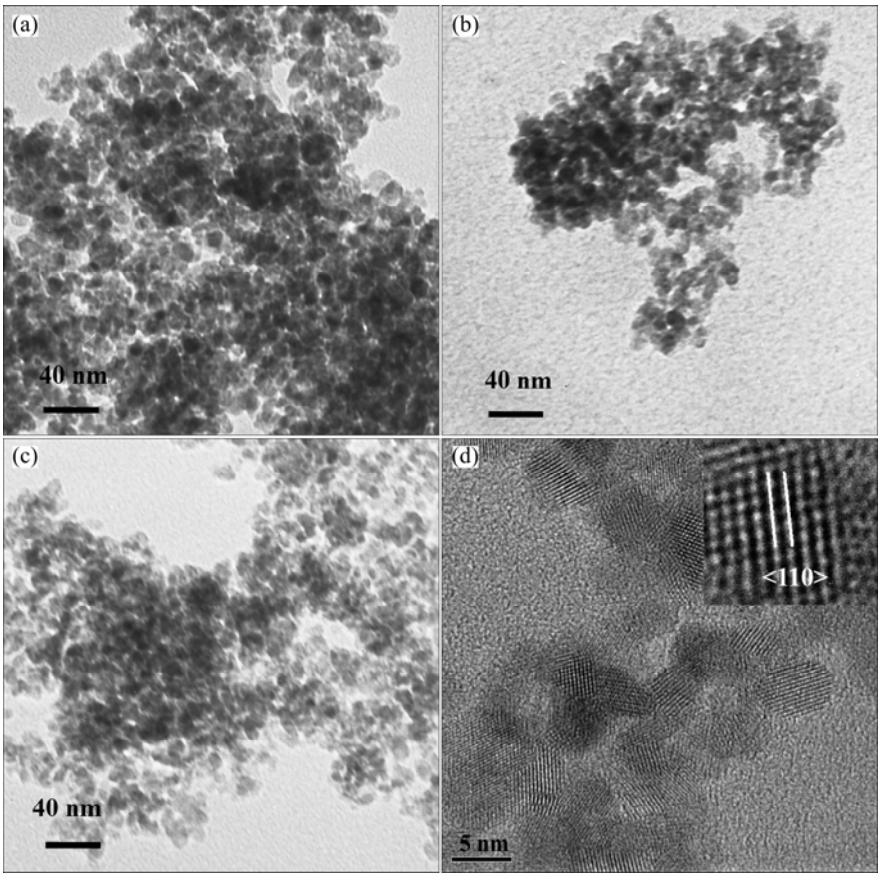

Fig. 3 Effects of aging temperature on SnO_2 nanoparticles: (a) TEM image, 25 °C; (b) TEM image, 70 °C; (c) TEM image, 110 °C; (d) HRTEM, 110 °C

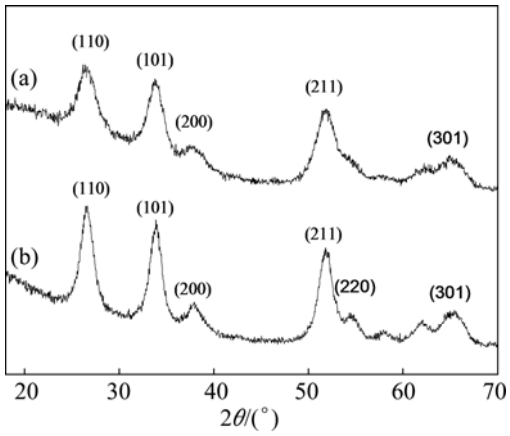

Fig. 4 XRD patterns of SnO_2 nanoparticles with size of 6.7 nm (a) and 16.2 nm (b)

The experimental results can be well interpreted by the above electrostatic-interaction mechanism. With rising Na_2SnO_3 concentration, the nucleation rate of H_2SnO_3 increases, resulting in the reduced particles size. The CTAB concentration in the experiment is sufficient to interact with the H_2SnO_3 sol so that its effect is negligible. At elevated aging temperature and prolonged aging time, the condensation degree of hydrous SnO_2 increases, leading to the reduction of particles size.

3.4 Photocatalytic activity

The as-prepared SnO_2 nanocrystals were employed as photocatalysts in the degradation of RhB solution. Figure 6(a) shows that, under UV irradiation and catalysis of SnO_2 nanocrystals (6.7 nm in size), the absorption of RhB solution declines with time and disappears completely after 80 min. Figure 6(b) shows the evolution of c/c_0 of RhB solution (i.e. the ratio of RhB concentration to its initial concentration). When UV irradiation was not provided, in the presence of SnO_2 nanocrystals, the variation of RhB concentration in 80 min can be neglected. When SnO_2 nanocrystals were not presented, under UV irradiation, the c/c_0 of RhB solution at 40 min was 58%. In the presence of SnO_2 nanocrystals and UV irradiation, for nanocrystals of 16.2 nm, 8.4 nm and 6.7 nm in size, the c/c_0 values of RhB solution at 40 min were 30%, 20% and 15%, respectively. That is, the catalytic activity of small nanocrystals is higher than that of large ones, which is ascribed to the high surface area of small nanocrystals [17]. For all the nanocrystals, the c/c_0 of RhB solution at 80 min is near zero.

The degradation mechanism of RhB under UV light is described as follows: when the energy (hv) of a photon matches or exceeds the bandgap of SnO_2, an electron (e^-)

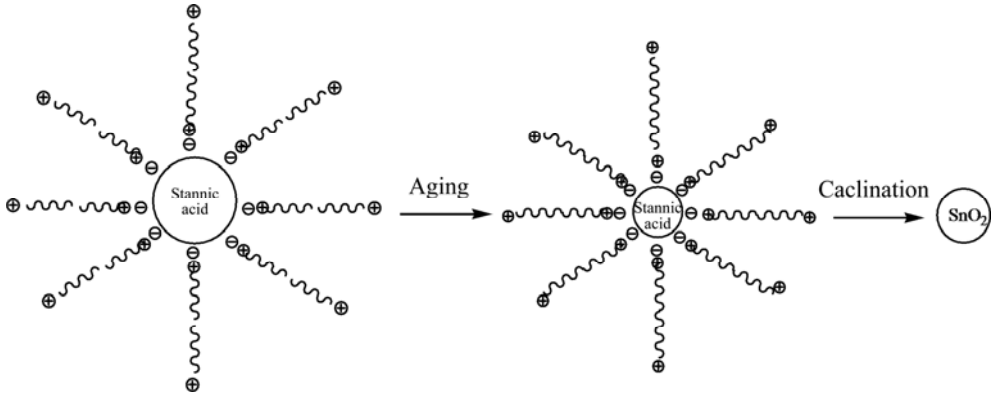

Fig. 5 Formation mechanism of SnO_2 nanocrystals

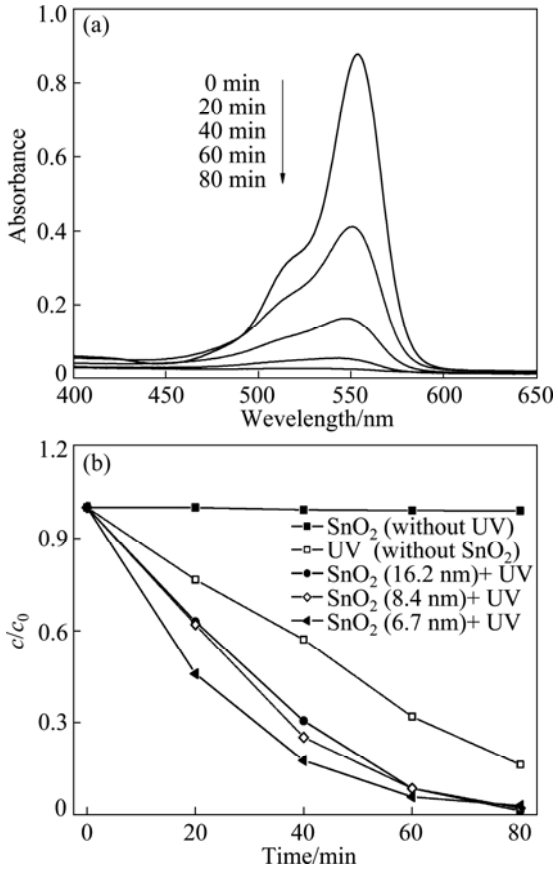

Fig. 6 Photocatalytic degradation of RhB solution: (a) Evolution of UV-vis absorption of RhB solution; (b) Change of RhB concentration

is excited from the valence band into the conductive band, generating a hole (h^+) [18]; then, oxidation agents (such as $\cdot O_2^-$, ·OH, ·OOH) are formed, which oxidize RhB molecules.

$$SnO_2+h\nu \rightarrow e^-+h^+ \quad (6)$$

$$H_2O+h^+ \rightarrow \cdot OH+H^+ \quad (7)$$

$$O_2+e^- \rightarrow \cdot O_2^- \quad (8)$$

$$\cdot O_2^-+H^+ \rightarrow \cdot OOH \quad (9)$$

$$RhB+h\nu \rightarrow RhB^* \quad (10)$$

$$RhB^*+O_2\,(or\cdot O_2^-,\ \cdot OH) \rightarrow degraded\ products \quad (11)$$

The high photodegradation rate of RhB in the presence of SnO_2 nanocrystals can be attributed to the generation of oxidative free radicals on the surface of SnO_2 nanocrystals.

4 Conclusions

Tin oxide nanocrystals stabilized with CTAB were synthesized by the Na_2SnO_3−CO_2 reaction system. With the increased Na_2SnO_3 concentration, elevated aging temperature and prolonged aging time, the size of SnO_2 nanocrystals decreases. The SnO_2 nanocrystals show high photocatalytic activities in the degradation of RhB solution. The catalytic activity of small nanocrystals is higher than that of large ones. A simple, cost-effective and versatile method for the preparation of SnO_2 nanocrystals was provided, as well as other weak-acidic metal oxide nanoparticles, such as Al_2O_3, SiO_2 and ZnO.

References

[1] GARRO R, NAVARRO M T, PRIMO J, CORMA A. Lewis acid-containing mesoporous molecular sieves as solid efficient catalysts for solvent-free Mukaiyama-type aldol condensation [J]. J Catal, 2005, 233: 342−350.

[2] LEITE E R, WEBER I T, LONGO E, VARELA J A. A new method to control particle size and particle size distribution of SnO_2 nanoparticles for gas sensor application [J]. Adv Mater, 2000, 12: 965−968.

[3] IDOTA Y, KUBOTA T, MATSUFUJI A, MAEKAW Y, MIYASAKA T. Tin-based amorphous oxide: A high-capacity lithium-ion-storage material [J]. Science, 1997, 276: 1395−1397.

[4] ZHANG Yue-lan, LIU Ying, LIU Mei-lin. Nanostructured columnar tin oxide thin film electrode for lithium ion batteries [J]. Chem Mater, 2006, 18: 4643−4646.

[5] CHOPRA K L, MAJOR S, PANDYA D K. Transparent conductors—A status review [J]. Thin Solid Films, 1983, 102: 1−46.

[6] BAYAL N, JEEVANANDAM P. Sol−gel synthesis of SnO_2−MgO nanoparticles and their photocatalytic activity towards methylene

blue degradation [J]. Materials Research Bulletin, 2013, 48: 3790−3799.

[7] BRIOIS V, BELIN S, CHALACA M Z, SANTOS R H A, SANTILLI C V, PULCINELLI S H. Solid-state and solution structural study of acetylacetone-modified tin(IV) chloride used as a percursor of SnO_2 nanoparticles prepared by a sol−gel route [J]. Chem Mater, 2004, 16: 3885−3894.

[8] JIANG Lu-hua, SUN Gong-quan, ZHOU Zhen-hua, SUN Shi-guo, WANG Qi, YAN Shi-you, LI Huan-qiao, TIAN Juan, GUO Jun-song, ZHOU Bing, XIN Qin. Size-controllable synthesis of monodispersed SnO_2 nanoparticles and application in electrocatalysts [J]. J Phys Chem B, 2005, 109: 8774−8778.

[9] LEITE E R, GIRALDI T R, PONTES F M, LONGO E, BELTRAN A, ANDRE J. Crystal growth in colloidal tin oxide nanocrystals induced by coalescence at room temperature [J]. Appl Phys Lett, 2003, 83: 1565−1568.

[10] MASUDA Y, OHJI W, KATO K. Highly enhanced surface area of tin oxide nanocrystals [J]. J Am Ceram Soc, 2010, 93: 2140−2143.

[11] EDUARDO J H L, CAUE R, ELSON L, EDSON R L. Growth kinetics of tin oxide nanocrystals in colloidal suspensions under hydrothermal conditions [J]. Chem Phys, 2006, 328: 229−235.

[12] RISTIC M, IVANDA M, POPOVIC S, MUSIC S. Dependence of nanocrystalline SnO_2 particle size on synthesis route [J]. J Non-Cryst Solid, 2002, 303: 270−280.

[13] WU Shui-sheng, CAO Hua-qiang, YIN Shuang-feng, LIU Xiang-wen, ZHANG Xin-rong. Amino acid-assisted hydrothermal synthesis and photocatalysis of SnO_2 nanocrystals [J]. J Phys Chem C, 2009, 113: 17893−17898.

[14] JUTTUKONDA V, PADDOCK R, RAYMOND J E, DENOMME D, RICHARDSON A E, SLUSHER L E, FAHLMAN B D. Facile synthesis of tin oxide nanoparticles stabilized by dendritic polymers [J]. J Am Chem Soc, 2006, 128: 420−421.

[15] ZEVENHOVEN R, ELONEVA S, TEIR S. Chemical fixation of CO_2 in carbonates: Routes to valuable products and long-term storage [J]. Catal Today, 2006, 115: 73−79.

[16] HOLLIDAY A K, HUGHES G, WALKER S M. Carbon in comprehensive inorganic chemistry [M]. Vol. I. Oxford: Pergamon Press, 1973.

[17] TALEBIAN N, JAFARINEZHAD F. Morphology-controlled synthesis of SnO_2 nanostructures using hydrothermal method and their photocatalytic applications [J]. Ceramics International, 2013, 39: 8311−8317.

[18] LI Jing-yi, MA Wan-hong, CHEN Chong-cheng, ZHAO Jin-cai, ZHU Huai-yong, GAO Xue-ping. Photodegradation of dye pollutants on one-dimensional TiO_2 nanoparticles under UV and visible irradiation [J]. J Mol Catal A, 2007, 261: 131−138.

SnO_2 纳米晶的制备及光催化性能

贾志谦[1]，孙慧杰[1]，王 妍[1]，甄甜丽[1]，常 青[1,2]

1. 北京师范大学 化学学院，北京 100875；
2. 装甲兵工程学院 再制造技术重点实验室，北京 100072

摘 要：以 Na_2SnO_3 和 CO_2 为反应物，十六烷基三甲基溴化铵(CTAB)为稳定剂，在温和条件下合成粒径小于 10 nm 的 SnO_2 纳米晶。CO_2 作为酸性气体，有利于精确调控 Na_2SnO_3 溶液的 pH 值，Na_2SnO_3 价廉且性质稳定，易于操作。研究 Na_2SnO_3 浓度、CTAB 浓度、熟化温度和熟化时间等对产物的影响。结果表明，随着 Na_2SnO_3 浓度的增加、熟化温度的升高和熟化时间的延长，粒径变小，粒子形成过程可由静电作用机理解释。SnO_2 纳米晶具有良好的光催化活性，且随着粒径的减小，其活性增大。

关键词：SnO_2 纳米晶；合成；光催化

(Edited by Hua YANG)